Research Article Adv. Mater. Lett. 2016, **7**(5), 344-348 Advanced Materials *Letters*

www.vbripress.com/aml, DOI: 10.5185/amlett.2016.6105

A first-principle study of the optical properties of pure and doped $LaNiO_3$

Tarun Kumar Kundu*, Debolina Misra

Department of Metallurgical and Materials Engineering, Indian Institute of Technology Kharagpur, Kharagpur 721302, India

*Corresponding author. Tel: (+91) 3222-2832-96; Fax: (+91) 3222-2822-80; E-mail: tkkundu@metal.iitkgp.ernet.in

Received: 21 August 2015, Revised: 06 December 2015 and Accepted: 24 March 2016

ABSTRACT

Density Functional Theory (DFT) is employed to study the various optical properties of pseudo-cubic $LaNiO_3$. As $LaNiO_3$ is a strongly correlated material, conventional DFT like LDA or GGA and even GW approximation fail to describe, we have examined the optical spectra of this compound using GGA(PBE)+U approach. The advantage of incorporating Hubbard *U* in this approach is to take the strong electronic correlation in the system into account. The optical spectra of this compound are found to be consisted of the Drude peak and some high energy peaks. While the Drude peak reflects the dominant free carrier contributions at the low energy region, the high energy peaks originate from the inter-band transitions within the system. We have also studied the remarkable changes in the optical properties in Fe doped $LaNiO_3$ ($LaNi_{1-x}Fe_xO_3$), in order to probe related properties, corresponding to their applications in solid-oxide fuel cells. Our calculations have revealed that even 25% of Fe doping is adequate to trigger a first order metal to insulator transition in $LaNiO_3$. The optical spectra of $LaNi_{1-x}Fe_xO_3$ compounds are calculated using the hybrid functional HSE and the doping-induced metal to insulator transition in $LaNiO_3$ is attributed to the altered crystal environment and electronic configuration of the compound. Copyright © 2016 VBRI Press.

Keywords: DFT; optical conductivity; doping; density of states; metal insulator transition.

Introduction

Materials exhibiting metal-insulator transitions (MIT) are of immense importance in the field of condensed matter physics due to their applications in Mottronics and non-volatile memory devices [**1-6**]. Change in electrical properties in some systems is often accompanied by a transition in the magnetic state also. MIT is generally seen in transition metal oxides and doped semiconductors [**7-10**]. The area of Mottronics which is considered to be one of the toughest challenges in the twenty first century relies on such systems which are prone to this kind of first order transitions. It has been observed that generally correlated materials have the tendency to undergo such MIT. In these materials the complex correlation between the structure and the electronic interactions trigger huge change in their physical properties when subjected to strain, pressure, doping, electric field, variation in temperature etc. which can change the carrier concentration within the compounds [**1, 7**]. Depending on the difference in resistivity in the two different phases (metallic and insulating), these materials are also used in switching devices and selectors in the array-type memory devices. Rare-earth nickelates ($RNiO_3$) is such a series of compounds where correlation plays a major role [**11, 12**]. The first member of this series namely $LaNiO_3$ has recently become very popular due to its metallic nature, while rests of the members of the series are insulators [**12**]. The importance of $LaNiO_3$ lies in its potential use in all the above mentioned fields, including its application as electrodes because of its metal-like behavior at room temperature [**13**]. Being the only conducting material in the series, although it never undergoes any MIT when subjected to temperature variation, a first order transition from metallic to an insulating state can still be obtained in this system by varying other parameters like strain, doping, oxygen-vacancy etc. [**13-19**]. The detailed understanding of this kind of transitions is necessary for its use in Mottronics, switching devices and for other suitable applications. Here we report the systematic theoretical investigation of the correlated metal $LaNiO_3$ we carried out using the density functional theory, and investigate how MIT can occur in the system as a function of appropriate substitution of Ni atom by Fe atoms. The changes in the optical spectra of $LaNiO_3$ due to the change in Ni content is analyzed and the various applications of Fe doped $LaNiO_3$ are discussed thereof.

Theory and computational details

$LaNiO_3$ is known to have a pseudo-cubic crystal structure with a small rhombohedral distortion [**12**]. In the cubic unit cell, the Ni atom occupies the body center position whereas the La and O atoms are at the corner and the face-center positions respectively. The structure optimization of cubic $LaNiO_3$ is carried out using the conjugant gradient algorithm, with force convergence of 0.01 eV/Å and energy convergence of 10^{-5}eV. A 520 eV plane wave cut off with a 5 × 5 × 5 k-mesh, centered at the Gamma point, is used to optimize the unit cell of $LaNiO_3$. The Gaussian scheme for Brillouin zone integration is used with a smearing width of 0.1 eV. All our DFT calculations are carried out using the MedeA-VASP (Vienna ab initio simulation package) software [**20**]. For $LaNiO_3$ we have calculated the optical properties e.g., optical conductivity, reflectivity, dielectric function, absorption index etc. to examine its metallic nature as well as the strong electron correlation it possesses. The optical properties of $LaNiO_3$ are calculated using different exchange functional to find out which one describes the correlated system most accurately. We have computed the density of states and all other optical constants of cubic $LaNiO_3$ using both the general DFT functional like local density approximation (LDA), generalized gradient approximation (GGA-PBE) and the DFT+U methods. These approaches differ in their ways of calculating the exchange-correlation energies. LDA is the simplest form of DFT calculation which takes the electron density around any point to be varying very slowly and considers the electron density at that point only. This approximation works well in case of homogeneous electron gas but fails in the real scenario, because electron density in any atom or molecule varies greatly as a function of position. This error is partially removed in the GGA approach which is a non-local method in the sense that, for each point a gradient is taken, and hence a small positional extent beyond that point of interest is considered [**21**]. However neither of these two methods is able to deal with strongly correlated system, as the Hamiltonian in both the cases do not incorporate the Hubbard *U* term. On the contrary, the DFT+U approach is the one which appropriately describes the electronic correlation in a system by taking an effective *U* which in turn includes both the Hubbard *U* and the Hund's coupling *J* [**22**]. However we have gone beyond DFT+U and used GW approximation (GWA) also, with Hubbard *U*. Standard GWA is carried out with our earlier GGA+U wave functions as the starting point. GWA is considered to be more precise compared to the early approaches and has been applied earlier to $LaMO_3$ (M=Ti~Cu) perovskites [**23**]. A comparison between the results obtained from these different approaches showed that the correlated metal $LaNiO_3$ is accurately described by the GGA+U approach which provides the best platform for dealing with a correlated material. It treats the effective electron interaction U_{eff} to be *U-J* to reproduce the correct ground states. We have taken the value of U_{eff} to be 3 eV and used the structural informations given in an earlier report to start our DFT calculations [**24**]. On the other hand, for the doped $LaNiO_3$ compounds, the hybrid functional HSE is found out to be an accurate method to describe the insulating states and the metal-insulator transitions [**25**]. First, super-cells are created from the parent $LaNiO_3$ and then appropriate substitutions of Ni by Fe atoms are made. It is observed that LDA, and GGA approaches fail to reproduce the insulating ground states of the doped $LaNiO_3$ compounds as they are unable to capture the band gaps in those compounds. Hence we have tried the hybrid functional method within DFT to address the Fe doped $LaNiO_3$ using HSE functional. The core idea of this approach lies in the concept of mixing a certain fraction of the DFT exchange and correlation term with the Hatree-Fock terms, which improves the accuracy of the results remarkably. In case of hybrid functional DFT, as the PBE0 approximation is computationally expensive to treat the long range exchange interaction in a metal, we have used the HSE functional which treats it in the short range level and is more effective in describing the energy gap in an insulator and a metal-insulator transition [**26**]. The detailed prescriptions for calculating different optical constants are discussed below in much detail.

All the optical constants are calculated from the complex dielectric function (ε). The imaginary part ε_i of the dielectric function ε is calculated first, using the relation following [**27**],

$$\varepsilon_i(\omega) = \frac{2e^2\pi}{V\varepsilon_0} \sum_{k,v,c} \left| \langle \psi_k^c | ur | \psi_k^v \rangle \right|^2 \delta\left(E_k^c - E_k^v - E\right)$$

where, Ψ_k^c, E_k^c, and Ψ_k^v, E_k^v, denote the wave functions and energies of conduction and valence bands respectively, *e*, ω, ε_0, and *V* are the electronic charge, frequency, dielectric constant in vacuum and the unit cell volume respectively, and the vector *u* here describes the polarization of the incident electric field. From the imaginary part of the dielectric function, the real part ε_r is extracted using the Kramers-Kroning transformation. The complex dielectric function can be expressed in terms of ε_r and the real part of the optical conductivity σ as follows [**27**],

$$\varepsilon = \varepsilon_r + \frac{4\pi i\sigma}{\omega}$$

Reflectivity and the absorption index are also calculated using the refractive index *n* and the extinction coefficient *k* which in turn are calculated from dielectric function ε. The reflectivity *R* and the absorption coefficient α in terms of *n* and *k* are defined as [**28**],

$$R = \frac{(n-1)^2 + k^2}{(n+1)^2 + k^2}$$

$$\alpha = \frac{2\omega k}{c}$$

In all the cases both the low frequency region $\omega\tau \ll 1$ and the high frequency region $\omega\tau \gg 1$ are extensively studied to analyze the exact ground state of the material as these two regions carry the signatures of two distinct conduction mechanisms within a solid. While the low frequency region is dominated by free carriers which are in abundance in a metal, the high frequency region is dominated by inter-band electronic transitions typical of a dielectric material. As in the limit $\omega\tau \ll 1$, both n and k become sufficiently large, hence in a metal,

$$R = 1 - \frac{2}{n} \rightarrow 1$$

In other words, a metal is characterized by its behavior as a perfect reflector and huge absorption coefficient in the low frequency region.

Results and discussion

Fig. 1 shows the calculated density of states for pure $LaNiO_3$ in different approaches. While LDA, GGA-PBE and GGA+U approaches yield more or less similar results, the GW+U differ from rest of them. $LaNiO_3$ is known to be a correlated metal with a quarterly-filled e_g band.

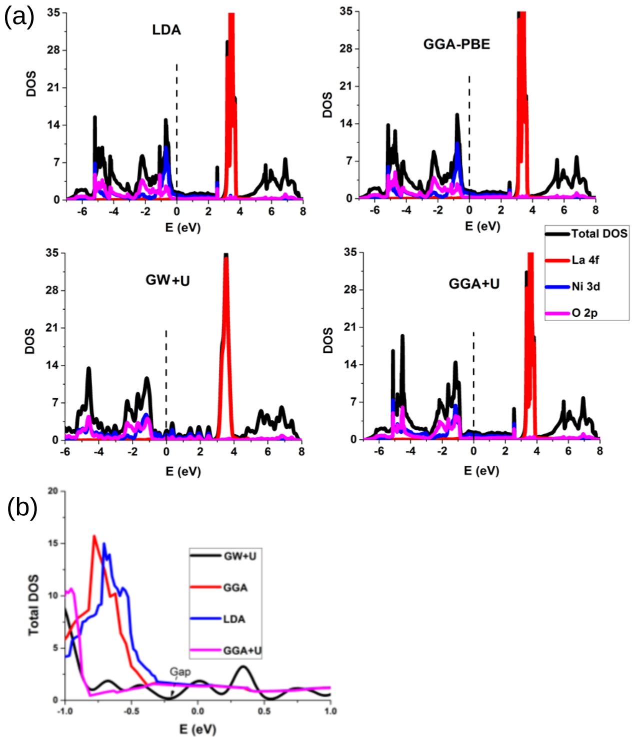

Fig. 1. Density of states for cubic $LaNiO_3$ using different DFT methods.

In all the cases in **Fig. 1** except the GW+U method, the position of the Fermi level clearly reveal the metallic nature of the system by finite density of states at the Fermi level. Our GW+U results match well with the earlier GW+U calculations applied on other perovskites [**23**]. However the above comparison indicates that as GW+U approach relies on the starting wave functions which are more localized than the other approaches, it is appropriate for describing those systems which are on the verge of electron localization. In case of $LaNiO_3$, GGA+U method seems to be the most accurate one to describe the metallic state retaining the electron correlation within the system. Hence regarding all the optical constants calculations afterwards, comparisons are made between LDA, GGA-PBE and GGA+U approaches only. The DOS of $LaNiO_3$ clearly show that there is a substantial hybridization between Ni 3d and O 2p orbitals, which corroborates the metallic ground state of the system. The real and imaginary parts of the complex dielectric function ε are calculated for cubic $LaNiO_3$ using different DFT functional and they are shown in **Fig. 2**. Both ε_r and ε_i follow the general trend of a metal which can be well explained by the classical Drude theory. With increase in energy, ε_r increases while ε_i decreases, and finally they reach zero in the high energy region, as expected in a metal. Our DFT results of the dielectric function of $LaNiO_3$ are in excellent agreement with previously reported theoretical and experimental results [**29-31**].

Fig. 3(a) shows the optical conductivity of $LaNiO_3$ in LDA, GGA-PBE and GGA+U approaches. Following the general trend, LDA overestimates the results and produces peaks with much higher intensities than the other approaches.

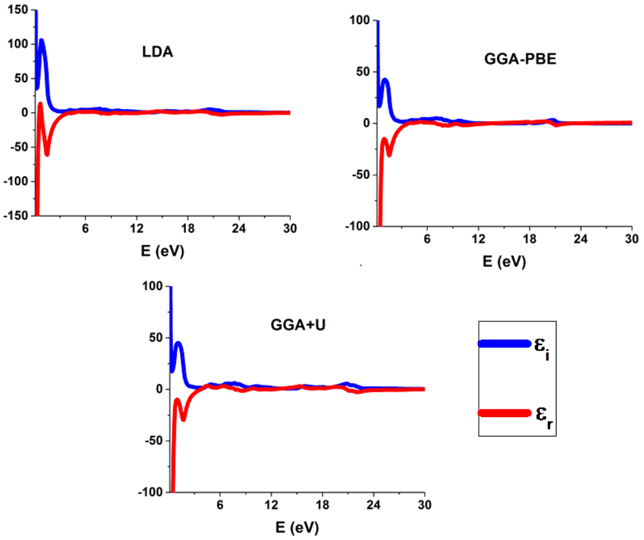

Fig. 2. Real and imaginary parts of the dielectric function of $LaNiO_3$ in different approaches.

While GGA-PBE and GGA+U methods yield more or less similar results in the low frequency region, they differ significantly in the high frequency region. Comparison of our theoretical results with experiments identifies GGA+U method to be the most relevant one to describe the correlated and metallic ground state of $LaNiO_3$. In all the cases, optical conductivity shows a distinct Drude peak which is typical of a metal and hence proves the metallic nature of $LaNiO_3$. Apart from the Drude peak, the optical conductivity has several peaks at higher energies starting from 1.5 eV. A careful analysis of the density of states of $LaNiO_3$ shows that these peaks owe their origin from different inter-band electronic transitions in the system. Our result is in excellent agreement with an earlier optical spectroscopic study of $LaNiO_3$ [**32**]. The most pronounced peak, situated at 1.5 eV originates from the electronic transitions between O 2p and Ni 3d states. While the peak at 4.2 eV is due to the transition between Ni 3d to La 4f and La 5d states, the high energy excitations at 5-5.5 eV are attributed to the transitions between O 2p and La 5d orbitals. The presence of both the Drude-peak which carries the signature of intra-band transitions and several inter-band transitions peaks gives rise to the complex conduction mechanism within the system. Refractive index n is also calculated using different approaches and is shown in **Fig. 3**(b). Similar effect is seen in the reflectivity spectra (**Fig. 3**(c)) of the system also. The low energy spectrum of bulk $LaNiO_3$ shows the system is a perfect reflector in the visible and IR range, which is the well-known property of a metal [**28**]. In the high energy region again several peaks emerge in the spectra showing the onset of inter-band electronic transitions. The calculations of the absorption spectra are also carried out as shown in **Fig. 3**(d). The large absorption coefficient of $LaNiO_3$ in the low frequency region identifies the system as a metal and indicates its potential application in infrared detectors [**33, 34**].

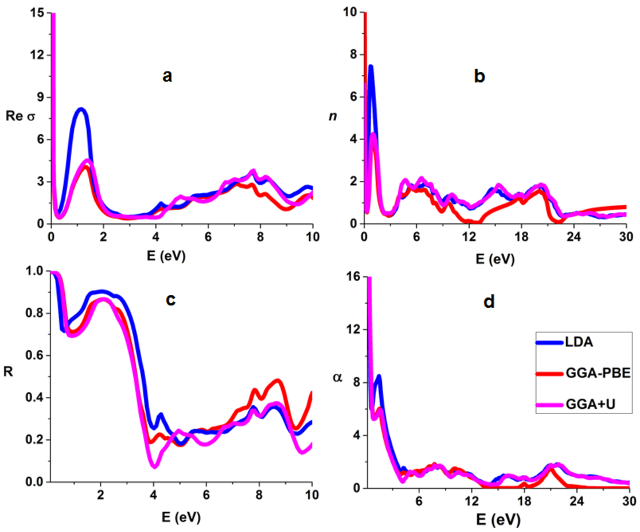

Fig. 3. (a) Optical conductivity and **(b)** refractive index **(c)** reflectivity and **(d)** absorption coefficient for cubic $LaNiO_3$ in different approaches.

In pure $LaNiO_3$, the Ni ion is trivalent and situated in an octahedral environment. When a small amount of Ni is substituted by equivalent Fe atoms, there is a considerable change in the crystal environment and a huge reduction of conductivity like an insulator is observed [**35, 36**]. The change is best demonstrated by the density of states and the optical conductivity spectra of the system. The density of states for $LaNi_{0.75}Fe_{0.25}O_3$using different approaches, are shown in **Fig. 4**.

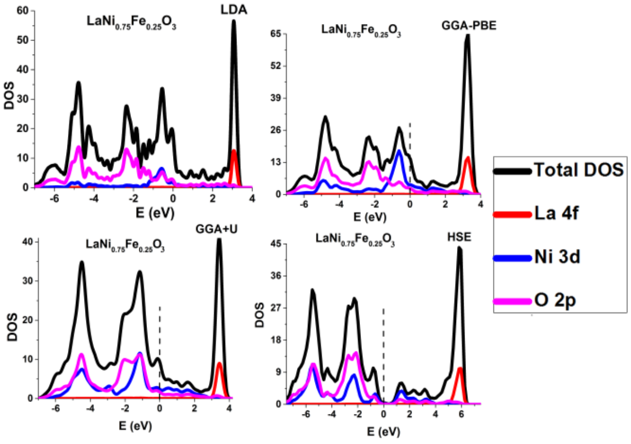

Fig. 4. Density of states for $LaNi_{0.75}Fe_{0.25}O_3$ using different DFT functional.

As LDA and GGA-PBE fail to describe the insulating ground state of the system, we have gone beyond that to adopt the hybrid functional approach, namely HSE. Our calculations indicate that substitution of 25 % Ni by Fe is enough to trigger the metal to insulator transition in $LaNiO_3$. While GGA-PBE approach can not reflect the insulating nature, the HSE hybrid functional correctly reproduced the insulating state of the system by showing an energy gap at the Fermi level (**Fig. 4**). The magnitude of the gap matches well with other available reports [**37**] and clearly indicates the onset of electronic localization within the material. The metal to insulator transition from $LaNiO_3$ to $LaNi_{0.75}Fe_{0.25}O_3$ can be explained from the optical conductivity spectra of these two compounds as shown in **Fig. 3** and **5**. While the presence of Drude peak in the optical conductivity spectra sows the metallic nature of $LaNiO_3$, the absence of Drude peak and the gap feature in the optical conductivity spectra of $LaNi_{0.75}Fe_{0.25}O_3$ demonstrates a metal to insulator transition due to Fe substitution. This metal to insulator transition in $LaNiO_3$, induced by small amount of Fe doping, can be viewed in terms of charge localization and reduced atomic overlaps in the material as some of the Ni ions are replaced by Fe ions. The differences between the electronic states of Ni and Fe ions are vital in analyzing the MIT in $LaNi_{1-x}Fe_xO_3$ compounds. In case of $LaNi_{1-x}Fe_xO_3$, the difference between the electronic spin configurations plays an important role in MIT. While Ni^{3+} ion is in low spin configuration ($t_{2g}^6e_g^1$) which prefers delocalization of the single *d* electron, Fe^{3+} is in high spin state ($t_{2g}^3e_g^2$) which is a stable configuration and prone to localization. Hence substitution of Ni by Fe reduces the itineracy of electron and promotes localization in the system. Apart from that, there is a bond length enhancement in the system as Fe^{3+} ions have larger radii compared to the Ni^{3+} ion. Increase in the ionic radii reduces the overlap between orbitals and hence promotes the insulating state over the metallic one.

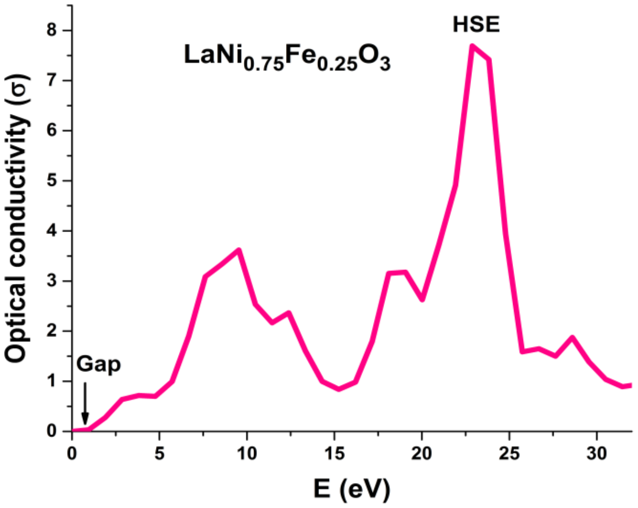

Fig. 5. Optical conductivity of $LaNi_{0.75}Fe_{0.25}O_3$, obtained within HSE method.

Conclusion

A detailed investigation of the optical properties of bulk $LaNiO_3$ is carried out using different DFT functional. While conventional DFT methods fail to describe strong correlation in a material, GGA+U approach is found to be the most appropriate one to describe the correlated metal $LaNiO_3$. The Drude peak and the high reflectivity of $LaNiO_3$ identify the system as a metal albeit correlated. When Ni ion is substituted by Fe ions even by 25 %, a first order MIT is observed. This transition is reflected clearly in the density of states and the gapped optical conductivity spectra of the doped systems. The Fe substitutions induced MIT in $LaNiO_3$ is then explained in terms of change in the electronic structure and reduction of orbital overlaps in the system.

Acknowledgements

We thank Ministry of Earth Science, Govt. of India (Project No.

MoES/16/48/09-RDEAS (MRDM5)), for the financial support to procure the server and the MedeA-VASP package.

Reference

1. Stefanovich, G.; Pergament, A.; Stefanovich, D.; *J. Phys.: Condens. Matter*, **2000**, *12*, 8837.
   DOI: 10.1088/0953-8984/12/41/310
2. Pergament, A.L.; Boriskov, P. P.; Velichko, A. A.; Kuldin, N. A.; *J. Phys. Chem. Solids*, **2010**, *71*, 874.
   DOI:10.1016/j.jpcs.2010.03.032
3. Nan, T.; Liu, M.; Ren,W.;Ye, Z. G.; Sun, N. X.; *Scintific Reports*, **2014**, *4*, 5931.
   DOI: 10.1038/srep05931
4. Ahn, C. H.; Triscone, J. M.; Mannhart, J.; *Nature*, **2003**, *428*, 1015.
   DOI:10.1038/nature01878
5. Son, M.; Lee, J.; Park, J.; Shin, J.; Choi, G.; Jung, S.; Lee, W.; Kim, S.; Park, S.; and Hwang, H.; *IEEE Electron Device Letters*, **2011**, *32*, 1579.
   DOI: 10.1109/LED.2011.2163697
6. Nandi, S. K.; Liu, X.; Venkatachalam, D. K.; Elliman, R. G.; *J. Phys. D: Appl. Phys.*, **2015**, *48*, 195105.
   DOI: 10.1088/0022-3727/48/19/195105
7. Limelette, p.; Georges, A.; Jerome, D.; Wzietek, P.; Metcalf, P.; Honig, J. M.; *Science*, **2003**, *203*, 89.
   DOI: 10.1126/science.1088386
8. Yang, Z.; Ko, C.; Ramanathan, S.; *Annu. Rev. Mater. Res.*, **2011**, *41*, 337.
   DOI: 10.1146/annurev-matsci-062910-100347
9. Cho, C. R.; Cho, S.; Vadim, S.; Jung, R.; Yoo, I.; *Thin Solid Films*, **2006**, *495*, 375.
   DOI: 10.1016/j.tsf.2005.08.241
10. Rosenbaum, T. F.; Milligan, R. F.; Paalanen, M. A.; Thomas, G. A.; Bhatt, R. N.; Lin, W.; *Phys. RevB*, **1983**, *27*, 7509.
    DOI:10.1103/PhysRevB.27.7509
11. Sarma, D. D.; Shanthi, N.; Mahadevan, P.; *J. Phys.:Condens. Matter*, **1994**, *6*, 10467.
    DOI: 10.1088/0953-8984/6/48/008
12. Piamonteze, C.; Tolentino, H. C. N.; Ramos. A. Y.; Massa, N. E.; Alonso, J. A.; Martınez-Lopes, M. J.; Casais, M. T.; *Physica Scripta*, **2005**, *115*, 648.
    DOI: 10.1238/Physica.Topical.115a00648
13. Son, J.; Moetakef, P.; LeBeau, J. M.; Ouellette, D.; Balents, L.; Allen, S. J.; Stemmer, S.; *Appl. Phys. Lett.*, **2010**, *96*, 062114.
    DOI: 10.1063/1.3309713
14. Sreedhar, K.; Honig, J. M.; Darwin, M.; Mcelfresh, M.; Shand, P. M.; Xu, J.; Crooker, B. C.; Spalek, J.; *Phys. Rev. B*, **1992**, *46*, 6382.
    DOI: 10.1103/PhysRevB.46.6382
15. Rajeev, K. P.; Shivashankar, G. V.; Raychaudhuri, A. K.; *Solid State Commun.*,**1991**, *79*, 591.
    DOI:10.1016/0038-1098(91)90915-I
16. Stewart, M. K.; Yee, C. H.; Liu, J.; Kareev, M.; Smith, R. K.; Chapler, B. C.; Varela, M.; Ryan, P. J.; Haule, K.; Chakhalian, J.; Basov, D. N.; *Phys. Rev B*, **2011**, *83*, 075125.
    DOI:10.1103/PhysRevB.83.075125
17. 17 Stewart, M. K.; Brownstead, D.; Liu, J.; Kareev, M.; Chakhalian, J.; Basov, D. N.; *Phys. Rev B*, **2012**, *86*, 205102.
    DOI: 10.1103/PhysRevB.86.205102
18. Dobin, A. Y.; Nikolaev, K. R.; Krivorotov, I. N.; Wentzcovitch, R. M.; Dahlberg, E. D.; Goldman, A. M.; *Phys. Rev B*, **2003**, *68*, 113408.
    DOI:10.1103/PhysRevB.68.113408
19. Scherwitzl, R.; Zubko, P.; Lichtensteiger, C.;Triscone, J. M.; , *Appl. Phys. Lett.*,**2009**, 95, 222114.
    DOI: 10.1063/1.3269591
20. Kresse, G.; Furthmuller, J.; *Phys. Rev. B*,**1996**, *54*, 11169.
    DOI:10.1103/PhysRevB.54.11169
21. Lewars, E.; Computational Chemistry; Springer, **2011**.
    DOI: 10.1007/978-90-481-3862-3
22. Gou, G.; Grinberg, I.; Rappe, A. M.; Rondinelli, J. M.; *Phys. Rev. B*, **2011**, *84*, 144101.
    DOI:10.1103/PhysRevB.84.144101
23. Nohara, Y.; Yamamoto, S.; Fujiwara, T.; *Phys. Rev. B*, **2009**, *79*, 195110.
    DOI:10.1103/PhysRevB.79.195110
24. Hamada, N.; *Phys. Chem Solids*, **1993**, *54*, 1157.
    DOI: 10.1016/0022-3697(93)90159-O
25. Von, V.; *All-Electron GW Calculations for Perovskite Transition-Metal Oxides*, Ph.D. thesis.
26. Franchini, C.; *J. Phys.: Condens. Matter*, **2014**, *26*, 253202.
    DOI: 10.10880953-8984/26/25/253202
27. Beal, A. R.; Hughes, H. P.; Liang, W. Y.; *J. Phys. C: Solid State Phys.*, **1975**, 19758.
    DOI:10.1088/0022-3719/12/5/017
28. Guan, L.; Liu, B.; Jin, L.; Guo, J.; Zhao, Q.; Wang, Y.; Fu, G.; *Solid State Commun.*, **2010**, *150*, 2011.
    DOI: 10.1016/j.ssc.2010.08.016
29. Berini, B.; Keller, N.; Dumont, Y.; Popova, E.; Noun, W.; Guyot, M.; Vigneron, J.; Etcheberry, A.; Franco, N.; and Silva, R. M. C. da.; *Phys. Rev. B*, **2007**, *76*, 205417.
    DOI: 10.1103/PhysRevB.76.205417
30. Hu, Z. G.; Li, W.W.; Li, Y. W.; Zhu, M.; Zhu, Z. Q.; Chu, J. H.; *Appl. Phys. Lett.*, **2009**, *94*, 221104.
    DOI: 10.1063/1.3148339
31. Zhu, J. J. ; Li , W. W.; Li, Y. W.; Shen, Y. D.; Hu, Z. G.; Chu, J. H.; *Appl. Phys. Lett*., **2010**, *97*, 211904.
    DOI:10.1063/1.3518493
32. Yu, J.; Sun, J. L.; Meng, X. J.; Huang, Z. M.; Chu, J. H.; Tang, D. Y.; Jin, C. Y.; Li, G.; Li, W. Y. ; and Liang, Q.; *J. Appl. Phys.*, **2011**, *90*, 2699.
    DOI: 10.1063/1.1394903
33. Hu, Z.; Meng, X.; Huang, Z.; Wang, G.; Zhao, Q.; and Chu, J.; *Jpn. J. Appl. Phys.*, 2003, *42*, 7045.
    DOI: 10.1143/JJAP.42.7045
34. Sarma, D. D. ; Chainani, A.; Krishnakumar, S. R.; Vescovo, E.; Carbone, C.; Eberhardt, W.; Rader, O.; Jung, Ch.; Hellwig, Ch.; Gudat, W.; Srikanth, H.; Raychaudhuri, A. K.; *Phys. Rev. Lett.*, **1998**, *80*, 4004.
    DOI:10.1103/PhysRevLett.80.4004
35. Ohzeki, T.; Hashimoto, T.; Shozugawa, K.; Matsuo, M.; *Solid State Ionics*, **2010**, *181*, 1771.
    DOI:10.1016/j.ssi.2010.09.041
36. Massa, N. E.; et. al., *Phys. Rev. B*, **1997**, *56*, 10178.
    DOI:10.1103/PhysRevB.56.10178